Tsunami Hazard Assessment of the Ocosta School Site in Westport, WA

Final Report: September 11, 2013

Supercedes February 24, 2013 Report

Frank González, Randy LeVeque and Loyce Adams
University of Washington

Westport, WA, Google Earth image. Blue rectangle is area of fine resolution GeoClaw tsunami model grid; white circle encompasses Ocosta School campus.

Study funded by Washington State Emergency Management Division

1 Background

The probability that an earthquake of magnitude 8 or greater will occur on the Cascadia Subduction Zone (CSZ) in the next 50 years has been estimated to be 10-14% (Petersen, et al., 2002). The last such event occurred in 1700 (Satake, et al., 2003; Atwater, et al., 2005) and future events are expected to generate a destructive tsunami that will inundate Westport and other Washington Pacific coast communities within tens of minutes after the earthquake main shock.

A previous study by Walsh, et al. (2000) documented evidence of two tsunamis that struck the Southwest Washington Coast, generated in 1700 and 1964 by earthquakes on the Cascadia Subduction Zone (CSZ) and Alaska-Aleutian Subduction Zone (AASZ), respectively. Tsunami simulations were conducted for two magnitude 9.1 (M9.1) CSZ earthquake scenarios, one of which included an area of higher uplift and, therefore, a higher initial tsunami wave offshore of northern Washington. These simulations resulted in moderate to high inundation of Washington coastal communities, including Westport, WA.

The Westport Ocosta School District is now proposing the construction of a new building to replace the current Ocosta Elementary School (Educational Service District 112, 2012). Since the Walsh et al. (2000) study, there have been significant advances in tsunami modeling and our understanding of potential CSZ earthquake events. Consequently, this study was commissioned and funded by the Washington Emergency Management Division to meet the need for an updated assessment of the tsunami hazard at the Ocosta School campus.

2 Earthquake Scenarios

In the general context of tsunami hazard assessment and emergency management planning, there are two general classes of tsunamigenic earthquake scenarios that represent quite different threats. A *distant*, or *far-field*, earthquake generates a tsunami that must traverse the open ocean for hours, generally losing a significant percentage of the destructive energy it had in the generation zone. In dramatic contrast, a *local*, or *near-field*, earthquake generates a tsunami that arrives at a nearby community in tens of minutes with much smaller loss of energy during the short propagation distance from the generation zone. This study considers tsunamigenic earthquake scenarios of each type.

The *local* or *near*-field M9 earthquake on the CSZ simulated in this study is the L1 scenario developed by Witter, et al (2011); it is one of 15 seismic scenarios used in a hazard assessment study of Bandon, OR, based on an analysis of data spanning 10,000 years. There is significant uncertainty in assigning an average return period to the L1 scenario, but based on a simple analysis of the evidence presented by Witter et al. (2011) on the estimated ages of M9 and larger CSZ earthquakes, a range of 1990-3300 years seems reasonable (Witter, 2013). The L1 scenario was chosen as the near-field source for this study because the standard engineering planning horizon for this project is about 2500 years and, in the professional judgment of the Witter et al. (2011) authors, L1 had the highest probability of occurrence of all the events considered with magnitude greater than M9. The length and width of L1 are approximately 1000 km and 85 km, respectively; salient features of the earthquake crustal deformation include subsidence at Westport of 1-2 m and a zone of about 8 to 10 m maximum uplift about 75 km offshore of Westport (Figure 1).

The distant or far-field M9.2 earthquake on the AASZ simulated for this study is similar to the 1964 Alaska event, which was the second largest worldwide since about 1900, when earthquake recordings began. The associated tsunami caused tremendous loss of life and property in Alaska and Crescent City, CA. This same scenario was developed and used in a previous study of Seaside, OR (Gonzalez, et al., 2009) and was also included in the Witter, et al. (2011) study of Bandon, OR. The Tsunami Pilot Study Working Group (TPSWG, 2006) estimated the mean return period of this scenario to be about 750 years.

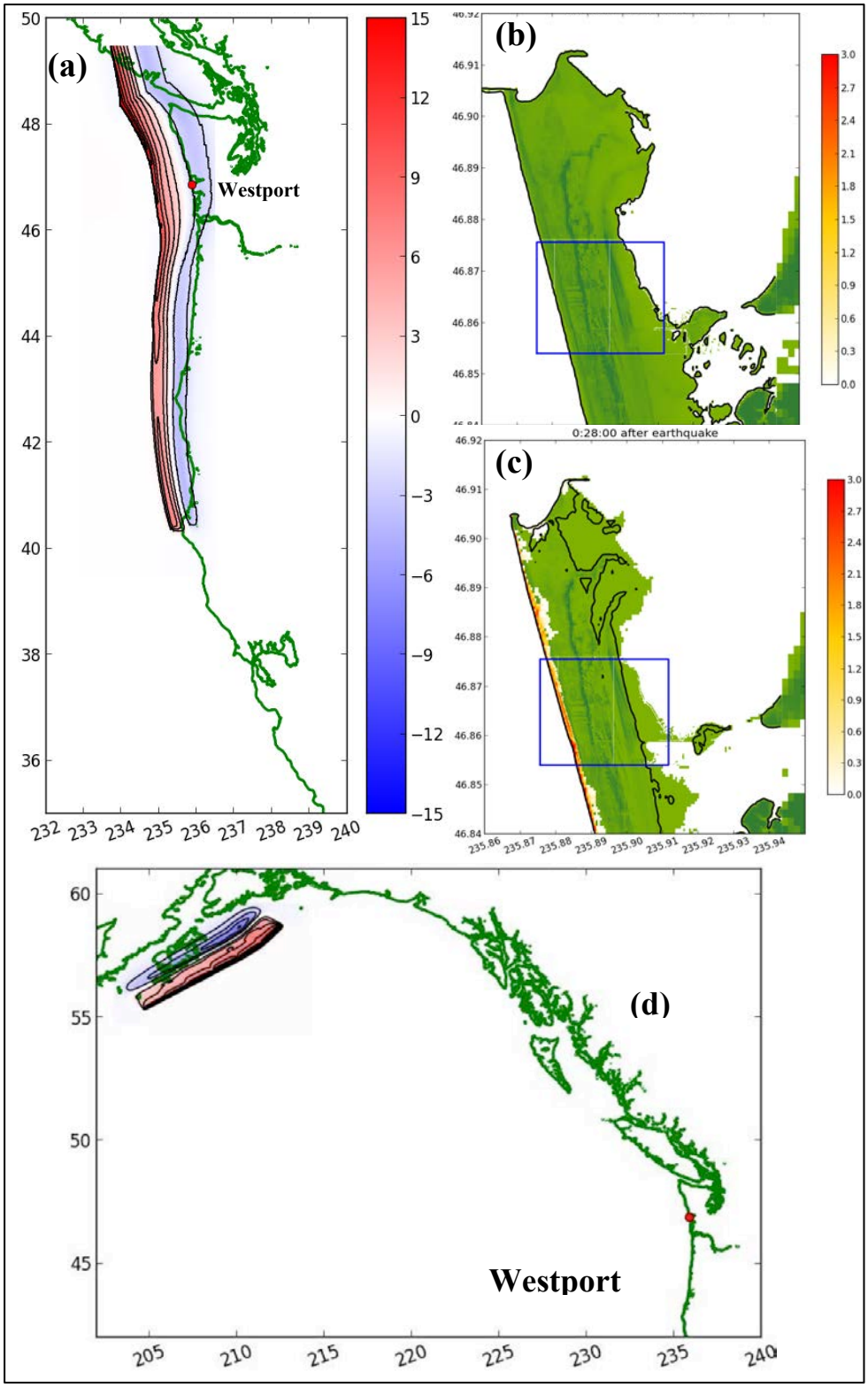

Figure 1. (a) CSZ earthquake vertical displacement, and initial tsunami waveform, in meters; note the coastal subsidence at Westport. (b) Black line is Westport mean high water (MHW) before CSZ event. (c) Black line is Westport MHW after subsidence. The blue rectangles are 7-10 m resolution computational grid areas that encompass the Ocosta school site. (d) AASZ earthquake vertical displacement, with vertical scale as in (a).

3 Tsunami Modeling and Results

GeoClaw Model

The simulations of tsunami generation, propagation and inundation were conducted with the GeoClaw model. This model solves the nonlinear shallow water equations, has undergone extensive verification and validation (LeVeque and George, 2007; LeVeque, et al., 2011) and has been accepted as a validated model by the U.S. National Tsunami Hazard Mitigation Program (NTHMP) after conducting multiple benchmark tests as part of an NTHMP benchmarking workshop (NTHMP, 2012).

Improved Bathymetric/Topographic Digital Elevation Model

A previous report, released on February 24, 2013 (previously available online but recently removed), utilized a bathy/topo DEM that was later found to be inaccurate. Inaccuracies in the topographic data were discovered while conducting modeling studies of a proposed vertical evacuation site at Long Beach, WA (González, et al., 2013). In particular, the NGDC Astoria V2 DEM (Love, et al., 2012) was not a bare earth product, because LIDAR topographic data collected in 2009 by Watershed Science (2010) were not incorporated. As a result, spurious North-South ridges were introduced between the Pacific Coast and the Ocosta school campus, and the height of existing ridges was overestimated (Figures 2 and 3); i.e., the number and height of ridges protecting the Ocosta site from tsunamis was overestimated. These inaccuracies did not affect the results obtained in the 24 February 2013 report for the AASZ earthquake scenario, because this far-field event did not create significant inundation at Westport (see Section 3.2, below). Potentially, however, the risk of Ocosta site flooding by the CSZ event is greater than previously reported. For this reason, additional simulations were conducted using a DEM developed from the 2009 LIDAR data by the Washington State Department of Natural Resources (DNR). **This report thus supercedes the February 24, 2013 report, which utilized an inaccurate DEM.**

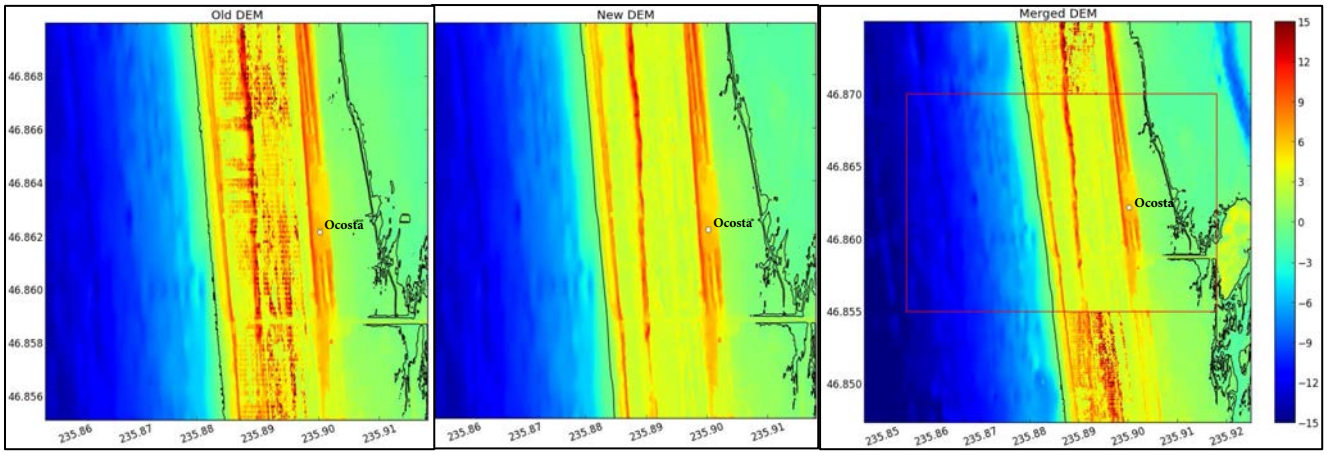

Figure 2. Left: Original DEM, in which the topography includes significant treetop and other features that rise above the bare earth level. Center: The LIDAR-derived DEM, in which the bare earth levels are more accurately represented. Right: The merged DEM used in these simulations, in which the LIDAR DEM (red rectangle) is embedded in a coarser grid. In the merged DEM, features that rise above bare earth are evident in the coarser grid DEM, but these are far enough removed from the Ocosta Elementary School campus that results at that site are not significantly affected.

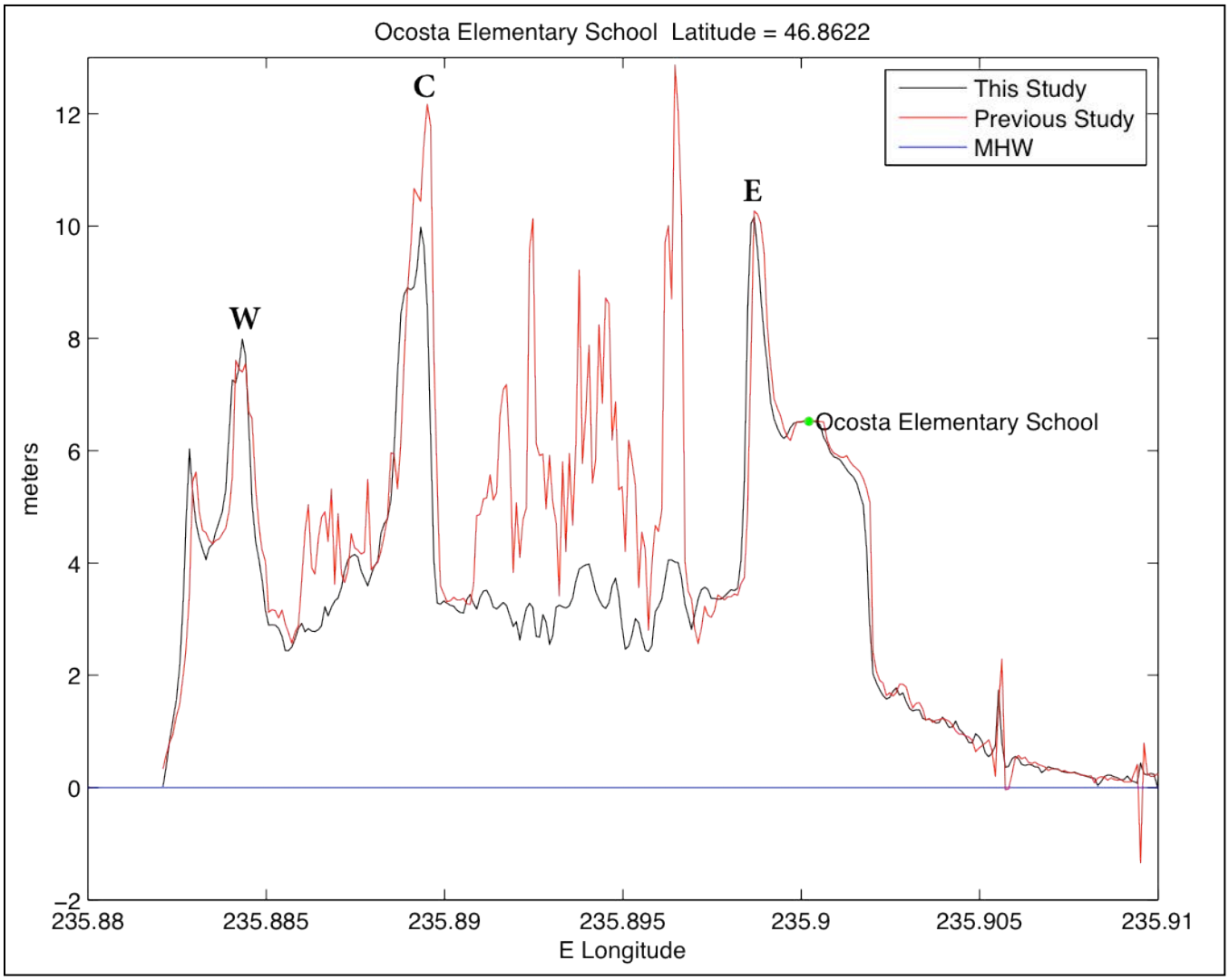

Figure 3. East-West transects of topography at the latitude of the Ocosta Elementary School. The three tallest ridges in the DEM of this study are labeled West (W), Center (C) and East (E), for reference. Note the spurious ridges, especially between the Center and East ridges, and the overestimated height of ridge C in the DEM of the previous study, in contrast to the "bare earth" LIDAR DEM of the present study.

Using this improved DEM, the sections that follow will present and discuss important features of the CSZ and AASZ scenarios described above, in terms of the tsunami hazard posed to Westport in general and to the Ocosta School site, in particular. In addition, we will discuss some inherent uncertainties in the specification of the earthquake scenarios, the limitations of the GeoClaw model, and the associated uncertainties in the results.

CSZ Simulation Parameters

Computations of tsunami flooding on the Ocosta School campus and surrounding area (the blue rectangle in Figure 1b) were made on a fine resolution computational grid of 1/3 arc-second; at the mean latitude of the study site, this corresponds to linear dimensions of approximately 7m x 10m in the East-West and North-South directions, respectively. All simulations were conducted with the tide level set to Mean High Water (MHW), which is standard practice for studies of this type.

A total of 5 simulations were conducted with the variations summarized in Table 1: two values of the Manning friction coefficient, a modification of the DEM as an ad-hoc erosion of three ridges to the west of the site, and an adjustment of the background sea level to reflect possible sea level rise.

Table 1. Summary of parameters for each of five CSZ simulations. See text for discussion of each parameter. The last column summarizes the depth of flooding at the center position of the circular-shaped Ocosta Elementary School building.

Simulation	Manning Coefficient	Ridge Erosion	SL Rise (m)	Flooding (m)
CSZ-1	0.025	No	0.0	0.00
CSZ-2	0.060	No	0.0	0.00
CSZ-3	0.025	Yes	0.0	0.47
CSZ-4	0.060	Yes	0.0	0.00
CSZ-5	0.025	No	0.5	0.00

The Manning coefficients of friction, *n*, of 0.025 and 0.06 correspond to gravelly earth and medium brush and trees (Chow, V.T., 1959). A sea level (SL) rise of 0.5 m was chosen for consistency with expected sea level rise (National Research Council, 2012) over the planned 75-year life of the school building. Erosion of ridges was addressed by the ad-hoc procedure of modifying the DEM to decrease their height, B (C. Ash, personal communication), according to:

$$B' = 6 \text{ m} \quad \text{if} \quad B > 6 \quad \text{for } x \leq 235.886$$

$$B' = 0.65\,B + 2.45 \quad \text{if} \quad B > 7 \quad \text{for } x > 235.866$$

where B' is the modified ridge height (Figure 4a).

3.1 Co-seismic Subsidence

Typically, subduction zone earthquakes are characterized by offshore uplift that generates the crest of an initial tsunami wave, nearshore subsidence that generates an initial tsunami wave trough offshore and coastal subsidence that can increase the depth of subsequent flooding on land. The initial wave splits in two; one wave propagates into the open ocean, the other propagates toward a coastal region that has now subsided and is therefore more susceptible to flooding. The AASZ earthquake is too far away to induce subsidence on the Washington coast, although subsidence does occur on the local Alaskan coastline (Figure 1d). In the near-field CSZ scenario modeled here, L1, the Westport peninsula is subjected to subsidence of about 2 m near the coast and increases to about 2.3 m farther inland (Figure 4b); interpolation implies subsidence at the Ocosta Elementary School site of about 2.1 m. To judge the uncertainty in this value, we first note that there are uncertainties in the specification of L1 discussed in Section 4.1 that propagates errors into subsidence estimates. We also note that an estimate of approximately 2 m subsidence is consistent with estimates derived from field data analyzed by Leonard et al. (2004) and Hawkes, et al. (2011) for the 1700 CSZ earthquake; however, the errors in the Leonard et al. (2004) and Hawkes et al. (2011) field observation databases were typically ± 0.5 – 0.8 m and ± 0.18 to 0.32 m, respectively. Furthermore, a comparison of field data with a number of elastic location models similar to source L1 of this study was made by Leonard et al. (2004) and the resulting error bars were also on the order of tens of centimeters. Therefore, the subsidence estimate of 2.1 m for the Ocosta Elementary School site must be considered to be uncertain to the same order, i.e. tens of centimeters.

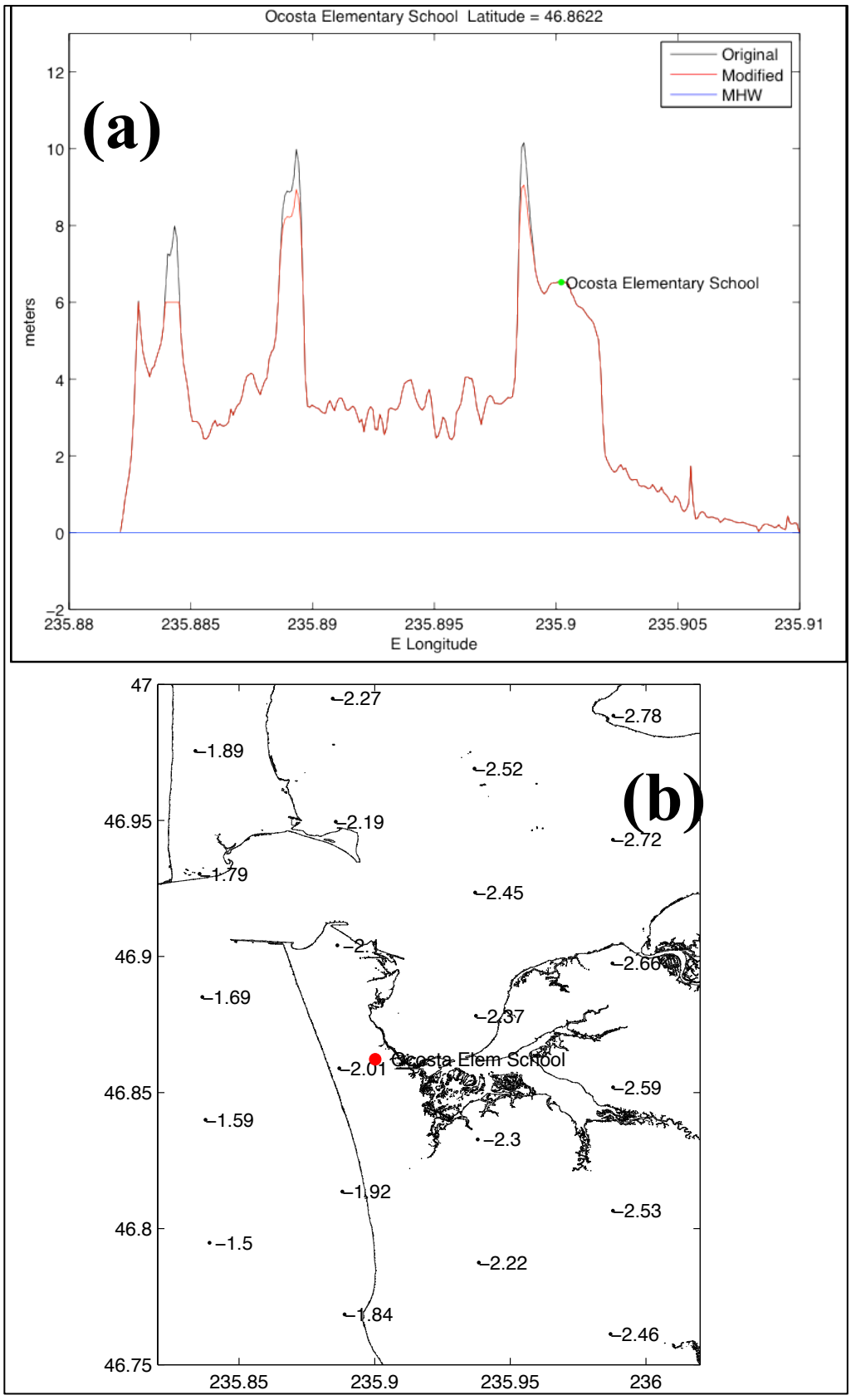

Figure 4. (a) East-West transects of original and modified topography through the Ocosta Elementary School site. The modified topography is intended to approximate the effects of erosion by an incident tsunami. **(b)** Subsidence, in meters, in the vicinity of the Ocosta Elementary School site.

3.2 Worst Considered Scenario CSZ-3 and the AASZ Scenario

Simulation CSZ-3 is the worst considered scenario. Figure 5 and the transect in Figure 6a were obtained by storing the maximum computed flood depth (i.e., "eta max," the depth of water above the local ground level) in each grid cell during the entire tsunami simulation; these figures show that flooding depth is in excess of 4.5 m on the coast and produces overtopping of the reduced-height ridges that floods the general area of the Ocosta School campus to a maximum depth of approximately 1.5 m. Note, however, that Figure 6b, a time series of flood depth, current speed and other important tsunami flow parameters, indicates a maximum flood level of about 0.47 m at a site centered on the circular-shaped Ocosta Elementary School. In contrast, the AASZ scenario produces coastal flooding of 3-5 m, but this is restricted to a narrow strip of the beach, with essentially no flooding of the residential areas to the east; there is also flooding of the Grays Harbor coast, but this does not reach the Ocosta campus.

Maximum current speed and arrival time are presented in Figure 7 for CSZ-3. On the Pacific coast, the tsunami arrives 20-25 minutes after the main shock of the earthquake, with current speeds in excess of 10 m/s; on the Ocosta school campus the initial arrival time of the tsunami is 35-40 minutes and maximum current speed is variable, but can be as great as 4 m/s. Note, however, that Figure 7 indicates that the maximum current speed is 1.15 m/s at a site centered on the Ocosta Elementary School building, and that the tsunami wave arrives about 36.5 minutes after the earthquake main shock. Such strong currents can be highly dangerous, demolishing structures and transporting logs, boats, automobiles and other rolling stock to form fields of debris that act as battering rams to multiply the destructive impact of the tsunami. In the AASZ scenario, arrival time computations (not shown) indicate that it takes the tsunami about 3.7 hours to traverse the Pacific and arrive at the Westport peninsula

.

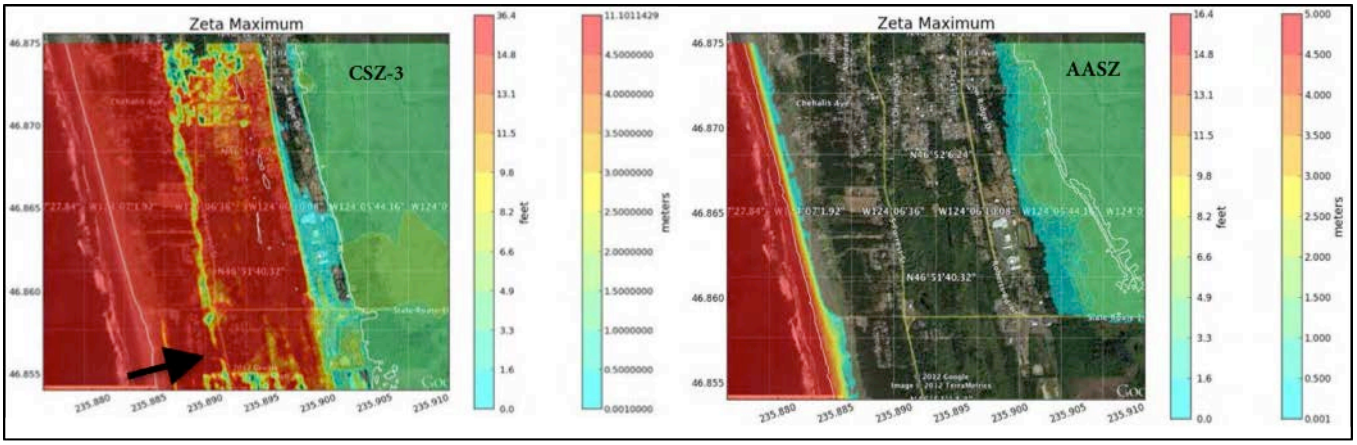

Figure 5. Maximum tsunami flooding depth for the worst considered case CSZ-3 (left) and AASZ (right) events. Note the maximum depths at the top of the vertical color scales: 11.4 m (37.6 ft) for the CSZ-3 event and 5.0 m (16.4 ft) for the AASZ event. The spatial resolution of the computational grid is1/3 arc-sec, or 7-10 m. The white lines are the coastline at MHW and the black arrow in the CSZ scenario (left panel) points to a relatively low area of ridge C that facilitates flooding to the east. Compare the new MHW coastline created by subsidence in the CSZ-3 scenario (left), with the original coastline, which does not subside in the AASZ scenario (right).

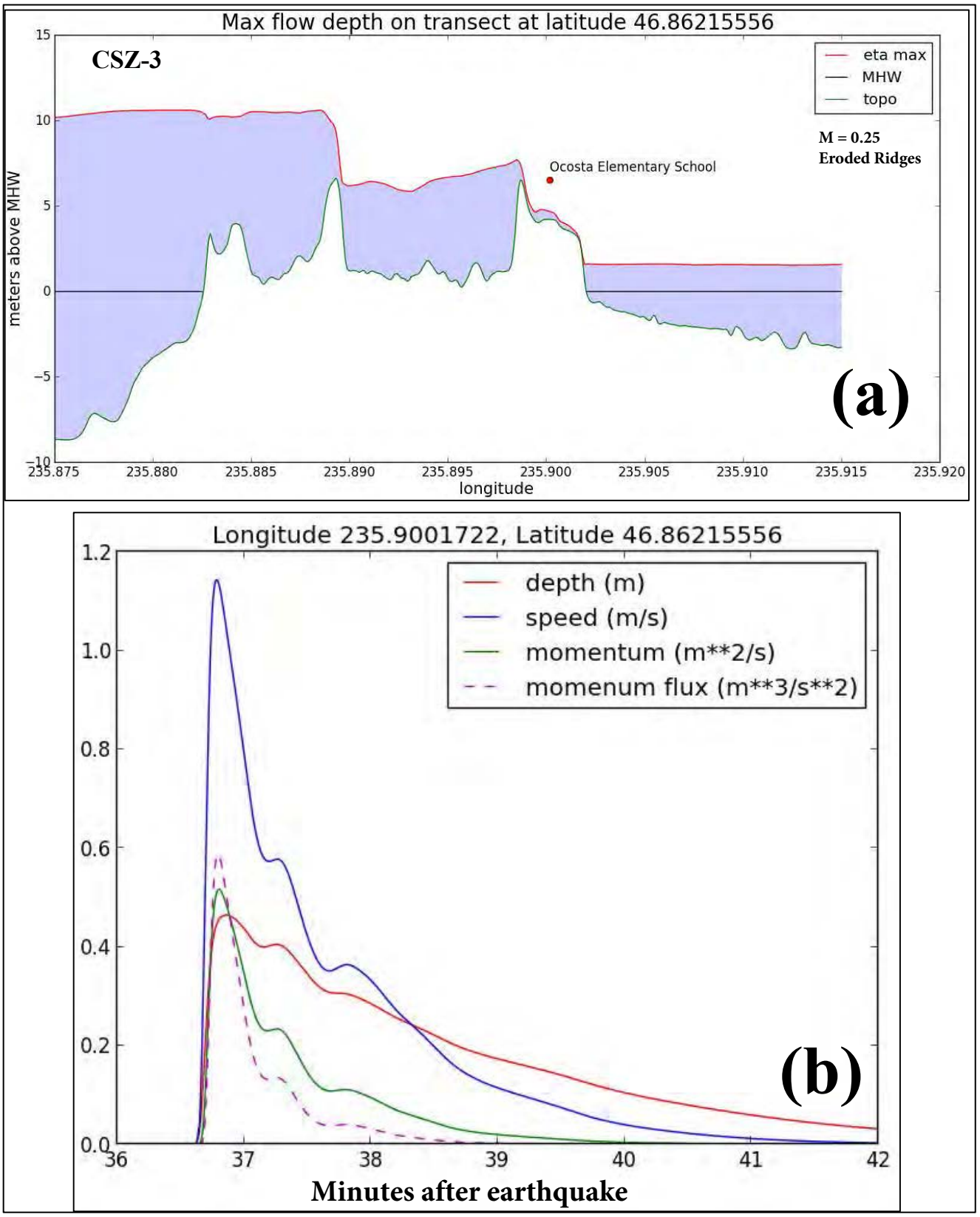

Figure 6. (a) East-West transect through the latitude of the Ocosta Elementary School. Vertical displacement of the school marker (red dot) reflects the approximately 2 m co-seismic subsidence at the site. **(b)** Tsunami flow parameters at a point centered on the Ocosta Elementary School building.

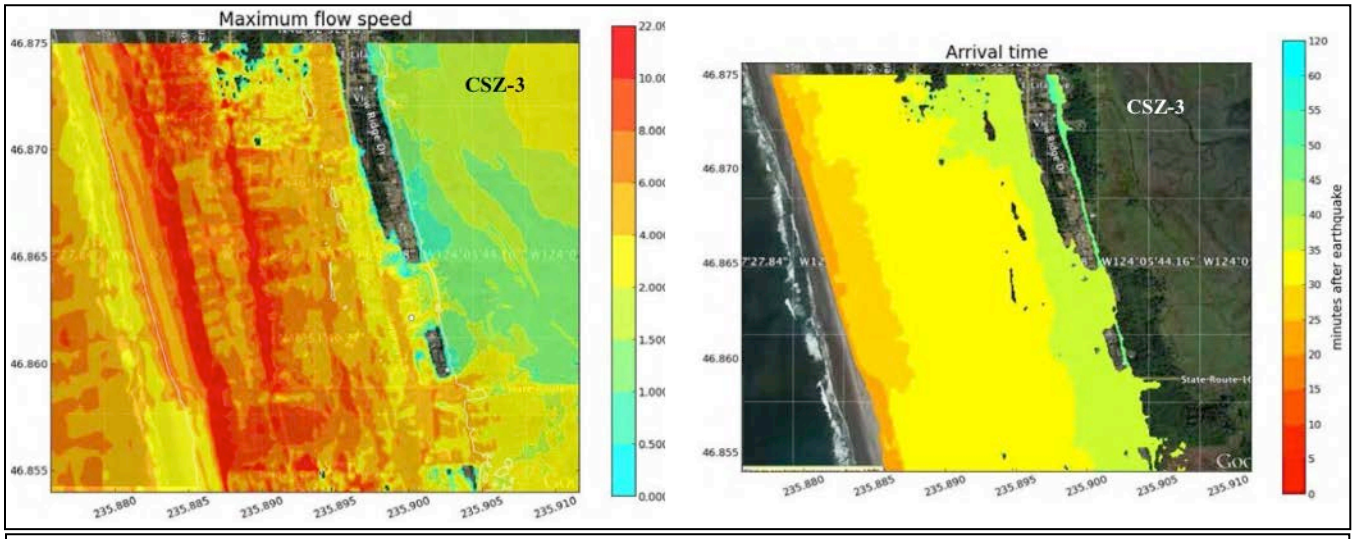

Figure 7. Maximum current speed and arrival time maps for scenario CSZ-3.

3.3 Additional CSZ Scenarios

Maximum flood depth maps and transects for the additional CSZ scenarios are presented in Figures 8 and 9. The effect of friction is clearly evident. In the two scenarios on the left, for which $n = 0.025$, the maximum wave heights are higher, the ridges are overtopped and some flooding occurs at the latitude of the Ocosta campus; the flooding is greater for CSZ-4, which assumes a sea level rise of 0.5 m. In contrast, the two scenarios on the right, with the higher value of friction, $n = 0.06$, produce lower maximum wave heights that do

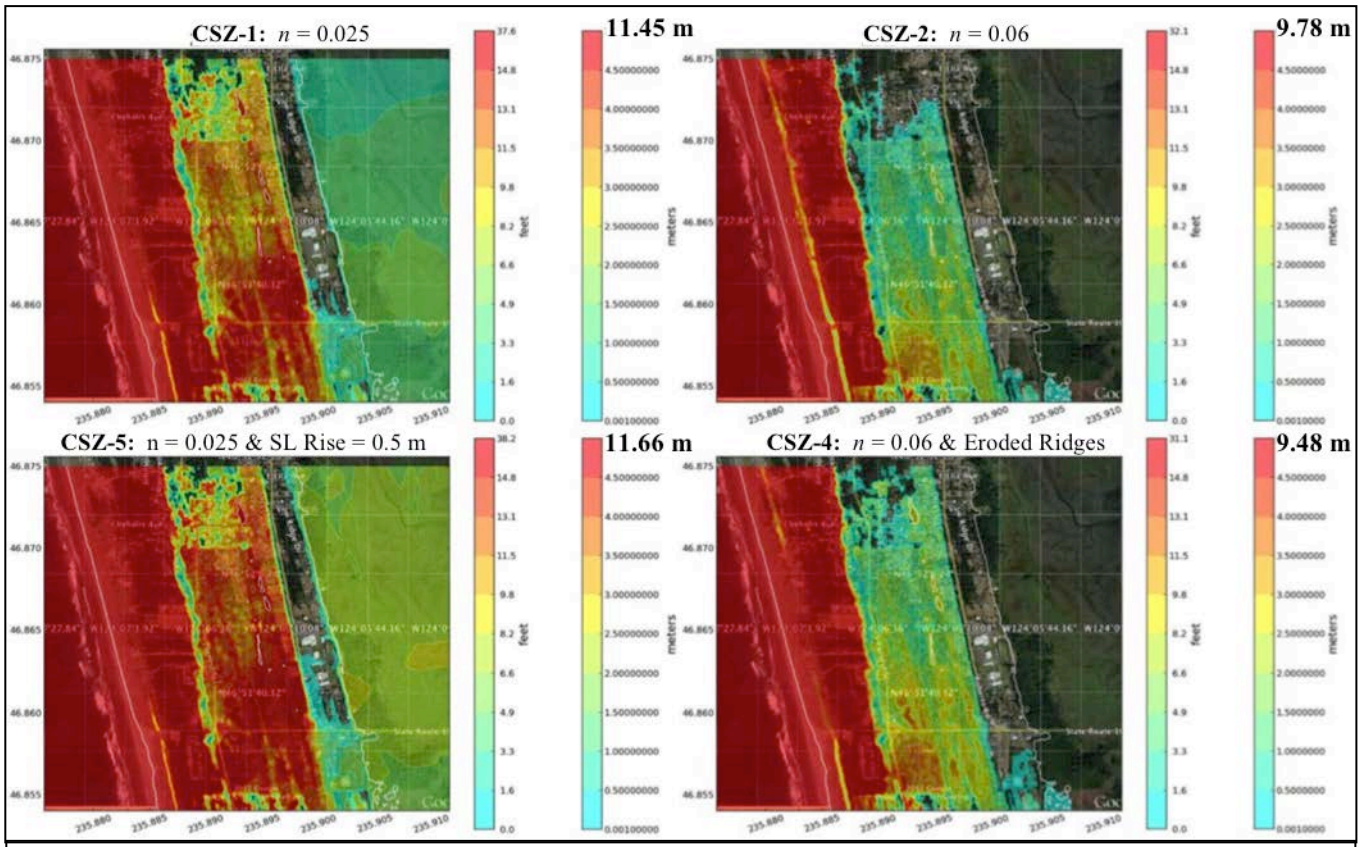

Figure 8. Maximum flooding maps for additional CSZ scenarios. Differences in the severity of flooding are due primarily to the effects of friction.

not overtop the ridges directly to the east and there is consequently no flooding of the Ocosta school

Maximum current speeds are presented in Figure 10. As would be expected, scenarios with a lower friction coefficient produce higher maximum speeds. Note also that, in Grays Harbor, although the tsunami wave height is low (Figure 8), it is accompanied by significant current speeds (Figure 10).

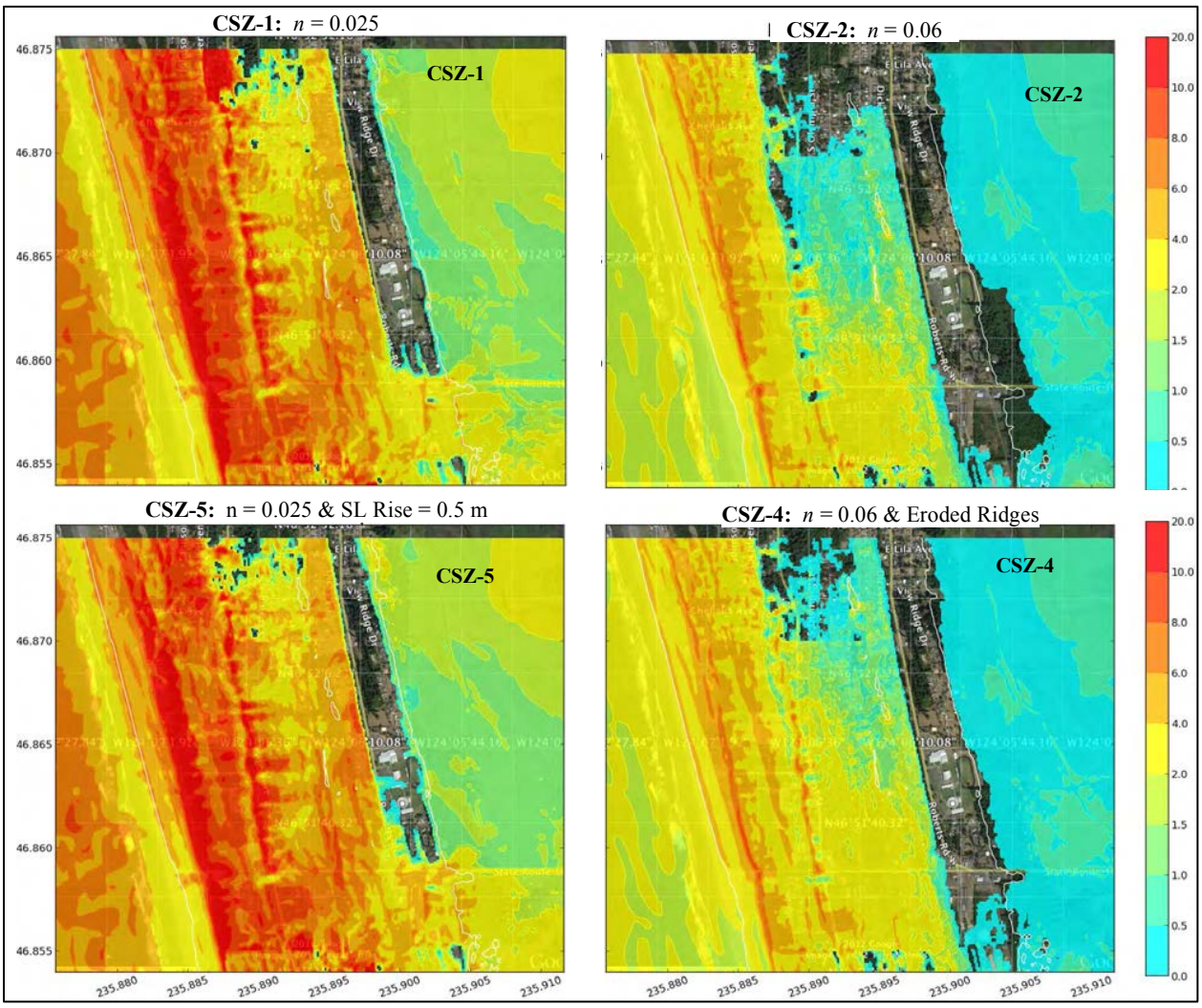

Figure 10. Maximum flow speed maps for additional scenarios.

4 Uncertainties and Limitations

Numerical models do not produce perfect simulations of any natural process. Here we discuss uncertainties and limitations most important to this specific study and, where possible, their probable influence on the model output.

4.1 Source Specification

This is likely the largest source of uncertainty in the study. Variations in the value of certain earthquake parameters can produce large differences in the subsequent tsunami flooding.

Earthquake Magnitude and Recurrence Interval

In general, the greater the earthquake magnitude, the larger the initial wave amplitude (but see the discussion of slip distribution uncertainty, below, for exceptions to this general rule). With regards to the CSZ event,

however, larger events would be associated with larger recurrence intervals than the estimated 1990-3300 years (Witter, 2013) and would be longer than the standard 2500 year planning horizon. In addition, Witter et al. (2011) estimate that "…the L1 scenario captures 95 percent of the hazard and more severe events are very unlikely."

The AASZ event is similar to a historic event, the 1964 Prince William Sound earthquake, and the magnitude was estimated from direct measurements. Such events are estimated to occur more frequently than great CSZ events, with a recurrence interval of about 750 years (TPSWG, 2006), but the threat to the Ocosta School campus from such great earthquakes is greatly mitigated by the large distance the tsunami must traverse to the site.

Earthquake Slip Distribution

The vertical displacement of the earth's crust presented in Figure 1 (a) is the direct result of a Pacific oceanic tectonic plate slipping (or subducting) beneath the North American continental plate, deforming both plates in the process. But the amount of slip is not distributed evenly on the common surface on which the two plates are in direct contact, known as the fault plane. There are patches on the fault plane, known as asperities, in which the two plates are more tightly locked by friction or protrusions of one plate into the other. But the relentless movement of the tectonic plates over decades and centuries continues to build up stress until the rock in the asperity region breaks and the plates slip past one another.

Most earthquake energy is released by the slip in asperities, and the larger the slip, the greater the earthquake energy. As a consequence, details of the slip distribution can make a significant difference in the initial amplitude of a tsunami; for example, if the slip is distributed evenly over the entire fault plane, then the initial tsunami amplitude will be about half the amplitude of a tsunami generated by slip distributed evenly over half of the fault plane. In particular, high slip values concentrated in an asperity region are associated with large values of vertical displacement of the ocean floor and a higher initial tsunami wave in the region.

Thus, the location of a coastal community relative to an asperity and the associated high wave region can have a direct effect on the severity of flooding in the community. When an earthquake is in the far-field, such as the AASZ scenario considered here, the earthquake resembles a point or line source and the details of the slip distribution are not important. However, details of the near-field slip distribution for the CSZ scenario L1 can have a significant affect on Westport inundation. For example, about 75 km northwest of Westport there is an offshore maxima of 10-12 m in crustal deformation and the initial tsunami waveform (Figure 1(a)); if this maxima was located closer to or farther from Westport, the inundation would likely increase or decrease, respectively. Similarly, if the concentration of slip (and therefore earthquake energy) resulted in a larger or smaller maximum value, then a corresponding increase or decrease in flooding would be expected. In addition to their effect on initial tsunami waveform, these uncertainties in slip distribution result in uncertainties in the amount of coastal subsidence (see Section 3.1, above). However, it is not possible to make a reliable prediction of slip distribution at this level of detail, and conducting numerical experiments to estimate the sensitivity of flooding to such changes is beyond the scope of this study.

Landslide sources

This study did not include modeling of local landslides that are triggered by earthquake shaking. The impact of tsunamis generated by landslides is restricted to the local generation area, so that this is not an important process in the case of a far-field event like the AASZ earthquake used in this study. However, submarine landslides offshore the Pacific and Grays Harbor coasts of Westport could increase the severity of flooding.

4.2 Model Physics

Certain values were assumed for important geophysical parameters, and some physical processes were not included in the simulations; their potential effect on the modeling results are discussed below.

Tide Stage

The simulations were conducted with the background sea level set to MHW and, in the case of CSZ-5, the additional assumption of long-term sea level rise of 0.5 m. Larger tide levels do occasionally occur, but the assumption of MHW is standard practice in studies of this type. These value are conservative, in the sense that less severe inundation results if sea level is set to a lower value.

Friction

The Mannings coefficient of friction in scenarios AASZ, CSZ-1, CSZ-3 and CSZ-5 was set to $n = 0.025$, a standard value used in tsunami modeling that corresponds to gravelly earth; scenarios CSZ-2 and CSZ-4 were simulated with a higher value, $n = 0.06$, corresponding to medium brush and trees (V.T. Chow, 1959). The value of 0.025 is conservative; the presence of trees and vegetation to the west and east of the Ocosta campus justifies the use of the larger value, 0.06, which has the effect of reducing flooding. However, large spatial variations occur in ground cover (e.g., pavement, gravel, brush, trees, etc.), but the model computations are conducted with a spatially constant value of Mannings coefficient of friction. A more realistic computation would use a spatially variable coefficient of friction, but the development of a grid representing spatially varying values of n is beyond the scope of this study. A limited test was conducted by developing the capability to assign a value of $n = 0.025$ and $n = 0.06$ to ocean and land cells, respectively; sea level was set to MHW (no sea level rise) and the ridges were reduced in height to approximate erosion. This was essentially scenario CSZ-4, but with friction of $n = 0.025$ for water cells, and the Ocosta campus flooding results were the same – although flooding was greater between ridges, there was no overtopping of the easternmost ridge and therefore no flooding of the Ocosta school campus.

Structures

Buildings were not included in the simulations. The presence of structures will alter tsunami flow patterns and, although local increases in flooding depth and current speed can occur when a tsunami wave encounters a structure, inland flow is generally impeded. Thus, the physical setting of this study is such that the inclusion of structures on the coast and farther inland toward the Ocosta School campus would generally reduce inland penetration of the tsunami, so that the lack of structures in the model is a conservative feature.

Debris

Large tsunamis inevitably create fields of debris that act as battering rams, multiplying the destructive impact. This process requires the expenditure of tsunami energy, which would tend to reduce the inland extent of the inundation.

Tsunami modification of bathymetry and topography

Severe scouring and deposition are known to occur during a tsunami, undermining structures and altering the flow pattern of the tsunami itself. This movement of material requires an expenditure of tsunami energy that tends to reduce the inland extent of inundation and thereby reduce the risk to the Ocosta campus. Scenario CSZ-3 included an ad-hoc procedure to reduce the ridge heights in the DEM, and this scenario turned out to be the worst considered. However, it must be noted that this ad-hoc procedure was static in nature, i.e., the hydrodynamics of the erosion process, in which tsunami energy is expended in reducing a ridge height by dislodging and transporting material, is not modeled; in that sense, then, the ridge reduction procedure used in this study should be considered conservative.

5 Discussion

Numerical simulations of Westport tsunami inundation by a far-field AASZ earthquake scenario produced no flooding of the Ocosta School campus. All five near-field CSZ scenarios listed in Table 1 inflicted severe flooding on the Pacific coast and much of downtown and residential Westport. Flooding of the Ocosta School campus did occur in the case of two scenarios, CSZ-3 and CSZ-5, characterized by assumptions of ridge erosion

and sea level rise, respectively. The worst case considered scenario was CSZ-3, producing values of maximum flooding depth on the overall Ocosta school campus up to1.5 m and maximum current speeds up to 4 m/s; however, at the specific site of the Ocosta Elementary school building, the maximum flooding and current speed were 0.47 m and 1.15 m/s, respectively. The primary source of uncertainty in these results is in the specification of the CSZ earthquake characteristics, especially the details of the seismic slip distribution; this leads to uncertainties in both the initial tsunami wave height and the degree of coastal subsidence and, therefore, uncertainty in the flooding depth and current speed. Since numerical experiments were not conducted to estimate the sensitivity of Ocosta campus flooding to these source uncertainties, it is impossible to rule out a future earthquake with a slip distribution that would result in greater flooding of the Ocosta school campus; it does seems likely, however, that the resulting increase caused by such an event would only be a modest fraction of the flooding simulated in this study. The hydrodynamics of physical processes such as wave/structure interaction, debris flow, scouring and deposition, were not included in the model. Because of the above uncertainties, the results should be used with caution.

References

Atwater, Brian F, Musumi-Rokkaku Satoko, Kenji Satake, Tsuji Yoshinobu, Ueda Kazue, and David K Yamaguchi (2005): USGS Professional Paper 1707, pp 1–144.

Chow, V.T. (1959): Open-channel hydraulics. New York, McGraw- Hill Book Co., 680 p.

Educational Service District 112 (2012): Facility Master Plan for the Ocosta School District, 68 pp, including 4 Appendices. (Available at http://www.ocosta.k12.wa.us/pages/Ocosta_School_District__172/Elementary_School_Bond)

Gonzalez, F I, E L Geist, B Jaffe, U Kânoğlu, H Mofjeld, C E Synolakis, V V Titov, et al. (2009): Probabilistic Tsunami Hazard Assessment at Seaside, Oregon, for Near- and Far-Field Seismic Sources, *Journal of Geophysical Research* 114 (C11) (November 24). doi:10.1029/2008JC005132.

González, Frank, Randy LeVeque, and Loyce Adams (2013): "Tsunami Hazard Assessment of the Elementary School Berm Site in Long Beach, WA." *UW Libraries ResearchWorks Digital Repository* (April 27): 1–13. http://hdl.handle.net/1773/22705 .

Hawkes, A. D., B. P. Horton, A. R. Nelson, C. H. Vane, and Y. Sawai (2011): Coastal subsidence in Oregon, USA, during the giant Cascadia earthquake of AD 1700, *Quaternary Science Reviews* 30 (3-4) (February 1): 364–376. doi:10.1016/j.quascirev.2010.11.017.

Leonard, L.J., R.D. Hyndman, S. Mazzotti (2004): Coseismic subsidence in the 1700 great Cascadia earthquake: coastal estimates versus elastic dislocation models. GSA Bulletin 116, 655-670.

LeVeque, J and D. L. George (2007): High-resolution finite volume methods for the shallow water equations with bathymetry and dry states. In P. L-F. Liu, H. Yeh, and C. Synolakis, editors, Advanced Numerical Models for Simulating Tsunami Waves and Runup, volume 10, pp 43-73. http://www.amath.washington.edu/ rjl/pubs/catalina04/.

LeVeque, R. J., D. L. George, and M. J. Berger (2011): Tsunami modeling with adaptively refined finite volume methods. Acta Numerica, pp 211-289.

Love, M.R., D.Z. Friday, P.R. Grothe, K.S. Carignan, B.W. Eakins, and L.A. Taylor (2012): Digital Elevation Model of Astoria, Oregon: Procedures, Data Sources and Analysis. Prepared for the Pacific Marine Environmental Laboratory (PMEL) by NOAA National Geophysical Data Center (NGDC), 30 pp.

National Research Council (2012): Sea-Level Rise for the Coasts of California, Oregon, and Washington: Past, Present, and Future. Washington, DC: The National Academies Press.

NTHMP (National Tsunami Hazard Mitigation Program) (2012): Proceedings and Results of the 2011 NTHMP Model Benchmarking Workshop. Boulder: U.S. Department of Commerce/NOAA/NTHMP (NOAA Special Report) 436 pp.

Petersen, M. D., C. H. Cramer, and A. D. Frankel (2002): Simulations of Seismic Hazard for the Pacific Northwest of the United States from Earthquakes Associated with the Cascadia Subduction Zone. Pure Appl. Geophys., 159, 2147-2168.

Plafker, George, K.R. Lajoie, and Meyer Rubin (1992): Determining recurrence intervals of great subduction zone earthquakes in southern Alaska by radiocarbon dating: in Taylor, R.E., Long, Austin, and Kra, R.S., eds., Radiocarbon After Four Decades: An Interdisciplinary Perspective, New York, Springer-Verlag, pp. 436-453.

Satake, Kenji, Kelin Wang and Brian F Atwater (2003): Fault Slip and Seismic Moment of the 1700 Cascadia Earthquake Inferred From Japanese Tsunami Descriptions, *Journal of Geophysical Research* 108 (B11): 1–17. doi:10.1029/2003JB002521.

TPSWG (2006): Seaside, Oregon Tsunami Pilot Study— Modernization of FEMA Flood Hazard Maps." *Joint NOAA/USGS/FEMA Report* (November 2): 1–176.

Walsh, T. J., C.G. Caruthers, A.C. Heinitz, E.P. Myers, III, A.M. Baptista, G.B. Erdakos, R.A. Kamphaus (2000): Tsunami hazard map of the southern Washington coast: Modeled tsunami inundation from a Cascadia Subduction Zone earthquake. Washington Division of Geology and Earth Resources Geologic Map GM-49, 1 sheet, scale 1:100,000, with 12 p. text.

Watershed Science (2010): "Lidar Remote Sensing Data Collection." *DOGAMI Report* (May 24): 1–25.

Witter, Robert C, Yinglong Zhang, Kelin Wang, George R Priest, Chris Goldfinger, Laura L Stimely, John T English, and Paul A Ferro (2011): Simulating Tsunami Inundation at Bandon, Coos County, Oregon, Using Hypothetical Cascadia and Alaska Earthquake Scenarios. *DOGAMI Special Paper 43* (July 11): 1–63.

Witter, Robert C. (2013): Personal Communication.